

Measurement of Cosmic-Ray H and He Isotopes in a Series of Annual Balloon Flights

J.Z. Wang¹, E.S. Seo¹, K. Anraku², M. Fujikawa², M. Imori², T. Maeno², Y. Makida³, N. Matsui², H. Matsumoto⁴, H. Matsunaga², J. Michell⁵, T. Mitsui⁴, A. Moiseev⁵, M. Motoki², J. Nishimura⁶, M. Nozaki⁴, S. Orito², J. Ormes⁵, T. Saeki², T. Sanuki², M. Sasaki⁴, R. Streitmatter⁵, J. Suzuki³, K. Tanaka³, I. Ueda², Y. Yajima⁶, T. Yamagami⁶, A. Yamamoto³, T. Yoshida³, K. Yoshimura²

¹*IPST, University of Maryland, College Park, MD 20742, USA*

²*University of Tokyo, Tokyo 113-0033, JAPAN*

³*KEK, Tsukuba, Ibaraki, 305-0801, JAPAN*

⁴*Kobe University, Kobe, Hyogo 657-8501, JAPAN*

⁵*NASA GSFC, Code 660, Greenbelt, MD20771, USA*

⁶*ISAS, Sagami-hara, Kanagawa 229-8510, JAPAN*

Abstract

The isotopes of cosmic-ray H and He have been measured by the Balloon Borne Experiment with a Superconducting Solenoid Spectrometer (BESS), which has been flown annually since 1993. We present here the absolute flux of ²H and ³He corrected to the top of the atmosphere. In the data analysis, the nuclear cross sections of H, He and their isotopes, which show strong energy dependence between 200 MeV/n and above 1 GeV/n, are critical for performing the efficiency corrections. These include corrections of nuclear interactions inside the BESS instrument, atmosphere attenuation, and atmospheric secondary particle production. The latest available cross section data and their parameterizations were utilized in the simulation code developed for this study.

1 Introduction:

The isotopes of cosmic-ray H and He are needed for understanding the propagation history of primary H and He nuclei in the galaxy. One of the high priority objectives of recent cosmic-ray experiments has been to determine the abundance of the rare isotopes ²H and ³He over a wide energy range. The Balloon Borne Experiment with a Superconducting Solenoid Spectrometer (BESS), which was flown annually since 1993, has been used to measure the cosmic-ray H and He and their isotopes. Monte-carlo simulations were used to fully understand the BESS instrument and to perform the spectra normalization. The available cross section data were compiled, and suitable hadronic packages for heavy ion simulations were selected for this study. In this paper, we present the absolute fluxes of H and He isotopes, ²H and ³He, measured from the first three flights (BESS 93, 94 and 95).

2 Simulations:

To achieve high precision measurement, redundant detection techniques were used in this experiment. See Yoshimura et al. (1995) and Moiseev et al. (1997) for the instrument details. The most important requirement in determining the absolute fluxes is knowledge of the detector efficiencies (e.g. the effective geometry factors). Monte-Carlo simulations are critical for understanding such a complicated experiment and obtaining pure and effective geometry factors. GEANT is a powerful code for tracking and simulating interactions of protons. Since GEANT does not accommodate simulation of heavy ions, we have had to compile cross sections and find suitable hadron simulation packages for heavy ion simulation. One of our choices for high energy hadronic collisions is FRITIOF, which is based on semi-classical considerations of string dynamics. With energy in the center-of-mass frame less than 5 GeV/n, where the string picture breaks down, FRITIOF is not applicable. Consequently another hadronic package, RQMD (Relativistic Quantum Molecular Dynamics), was adopted in our simulations for H and He isotopes.

2.1 Inelastic cross sections: Since there was a significant amount of material along the tracks of particles through the BESS instruments (the total thickness traveled by a typical incident particle to trigger the instrument is 17.8 g/cm^2 of instrument materials and 5 g/cm^2 of atmosphere), the nuclear interaction loss significantly influences the effective geometry factors.

The most important input for the simulations is the inelastic cross sections of ^2H and ^3He particles with the materials of the BESS instrument. Figure 1 shows that the nuclear inelastic cross sections of ^2H and ^3He on a hydrogen target has a strong energy dependence below a few GeV per nucleon.

A parameterization method is needed for calculating the cross section of a particle interacting with different BESS materials at different energies. The Langley Research Center (LaRC) model, which was developed by Tripathi et al. (1996), was selected for our simulation study. It is an universal parameterization method for absorption cross sections, and it can be used for any system of colliding nuclei in the energy range from a few MeV/n to a few GeV/n. In the LaRC model, the reaction cross section σ_R can be expressed by the formula

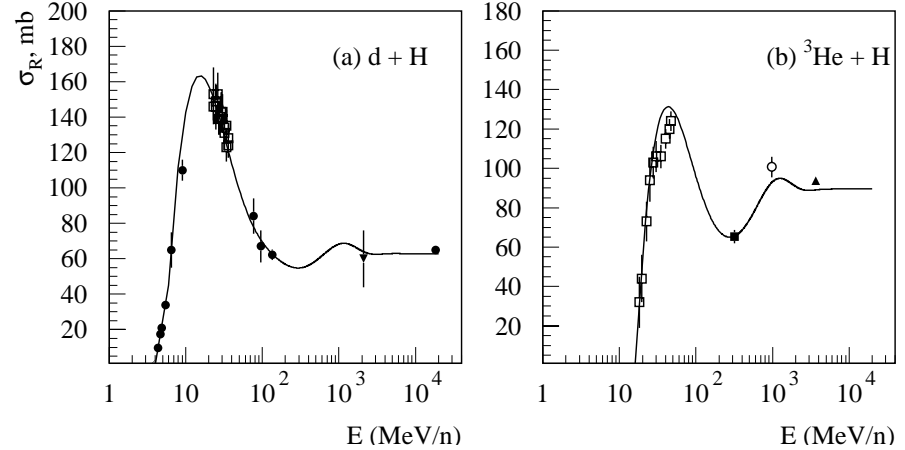


Figure 1: Inelastic cross section of (a) ^2H and (b) ^3He on a hydrogen target with the LaRC parameterization. Data points are as follows: filled circles, Meyer (1972); open squares, Carlson (1996); downward pointing triangle, Jaros et al. (1978); filled square, Blinov et al. (1984); open circle, Blinov et al. (1985); upward pointing triangle, Glagolev et al. (1993)

where $r_0 = 1.1 \text{ fm}$, A_p and A_t are the projectile and target mass numbers, and E_{cm} is the colliding system center-of-mass energy. The δ_E term represents two effects: transparency and Pauli blocking at intermediate and higher energies. The last term is the Coulomb interaction term with B as the energy dependent Coulomb barrier. As shown in Figure 1, our compiled data agree well with the LaRC model calculation (Solid curves).

2.2 Effective geometry factors: With GEANT/GHEISHA, we set up the code for the BESS instrument and performed the simulation for protons. For heavy ion simulations, two interfaces were made. One was to implement the LaRC model to determine the interaction probabilities of heavy ions, and another interface was used to connect RQMD/FRITIOF with GEANT to perform the heavy ion simulation. The delta ray effect was demonstrated to significantly influence the high charge and high energy simulations of BESS (Seo et al., 1998). In this study, the delta rays were simulated explicitly with threshold above 100 keV. The simulation results for the effective geometry factors of ^2H and ^3He are shown in the Fig. 2. Compared with the raw geometry factors (dashed line) of $0.42 \text{ m}^2\text{sr}$ for BESS 93 and 94 ($0.32 \text{ m}^2\text{sr}$ for BESS 95), the difference shown in the figure is the geometry factor loss due to ionization, nuclear interactions, and delta ray effects.

Figure 2 shows the effective geometry factor (GF) in m^2sr versus kinetic energy in GeV/n. The y-axis ranges from 0 to 0.5, and the x-axis is logarithmic from 10^{-1} to 10. A dashed horizontal line at $0.42 \text{ m}^2\text{sr}$ represents the raw geometry factor. Two data series are shown: ^2H (filled circles) and ^3He (filled triangles). Both series show a peak around $0.35 \text{ m}^2\text{sr}$ at 0.1 GeV/n and then decrease towards $0.3 \text{ m}^2\text{sr}$ at 1 GeV/n .

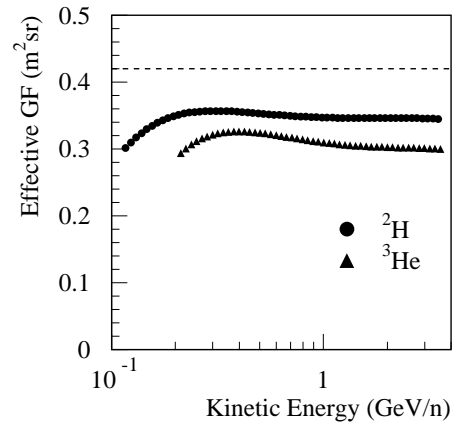


Figure 2: The BESS 93 effective geometry factors of ^2H and ^3He

3 Analysis:

3.1 Data selection: The unbiased count-down data were used in this analysis (see Yoshimura et al., 1995; Seo et al., 1997). Three kinds of event selection criteria were applied for both low threshold and high threshold data sets: (a) single track cuts, (b) track quality cuts, and (c) consistency cuts. See Seo et al. (1998) for details of the cuts. The H and He candidates were selected by the single track cuts and the dE/dx cuts. Events with nuclear interactions in the BESS instrument were removed by the single track cuts. The efficiency of the single track cuts were calculated with the Monte-Carlo simulation described in the above section. The later two cuts (b) and (c) were used to select events with high precision of rigidity and velocity measurement. For charge $Z=1$ and 2 particles respectively, the efficiencies were 70% and 63% for BESS 93, 57% and 65% for BESS 94, and 60% and 57% for BESS 95. The H and He isotopes were separated by the same mass histogram method used in BESS 93 data analysis (Seo et al., 1997).

3.2 Atmospheric corrections: The atmospheric corrections included two parts: (a) atmospheric attenuation and (b) secondary particle production. The attenuation loss was calculated with Monte-Carlo simulations. The particle loss fractions due to nuclear interaction in the 5 g/cm² atmosphere were 8% for ²H and 12% for ³He, with little energy dependence. These results are consistent with the fractions calculated by using the attenuation lengths of 75 g/cm² for ²H and 40 g/cm² for ³He (Davis et al., 1995).

In balloon experiments secondary particles produced in the atmosphere will be measured in addition to the primary cosmic-rays. Secondary corrections become very important to get the cosmic-rays spectra at the top of the atmosphere, especially for the rare isotopes like ²H and ³He. Secondary corrections for ²H and ³He are sensitive to the flux of primaries (proton and ⁴He, etc.). The BESS 93, 94 and 95 primary proton and ⁴He spectra, which were measured simultaneously, were used in this calculation. Refer to Seo et al. (1997) for the calculation procedure.

3.3 Flux and Uncertainties: The count spectra $N(E)$ of selected H and He isotopes were normalized to the final energy spectra. The differential fluxes at the top of the atmosphere as a function of kinetic energy per nucleon, E , are given by

$$F_{TOA}(E) = \left(\frac{N(E)C_d}{E_{gf}(E)E_cT\Delta E_{in}} - f_{sec}(E) \right) \frac{\Delta E_{in}}{\eta(E)\Delta E_{TOA}} \quad (2)$$

where C_d is the inverse of the count-down rate, $E_{gf}(E)$ is the energy-dependent effective geometry factor, E_c is the efficiency of the data selection cuts, T is the live time, ΔE_{in} is the bin size inside BESS and corresponds to ΔE_{TOA} at the top of the atmosphere, $\eta(E)$ is the correction factor of attenuation loss, and $f_{sec}(E)$ is the atmospheric secondary spectra.

The uncertainties of the final spectra come from several aspects: statistics, mass separation, effective geometry factors, atmospheric attenuation, and secondary production. Assuming these uncertainties are uncorrelated, we estimated that the uncertainties involved in our final spectra range from 12% to 26% for ²H and from 11% to 20% for ³He. The uncertainties are higher at both low and high energies. At low energy, the uncertainty mainly comes from secondary correction. At high energy, it is more difficult to separate isotopes from primaries. Consequently the corresponding uncertainty becomes higher.

4 Results:

The absolute fluxes of H and He isotopes, ²H and ³He, obtained by analyzing the BESS data are shown in Fig. 3(a) and 3(b), respectively. Only statistical uncertainties are included in the error bars shown in the figure. A successive evolution of fluxes along with the solar modulation are clearly shown in the energy spectra measured by BESS 93, 94, and 95. The solid curve is a theoretical prediction based on the reacceleration model with modulation parameter 600 MV (Seo et al., 1997). Our resulting spectra are consistent with both previous observations at low energies and with the theoretical calculations.

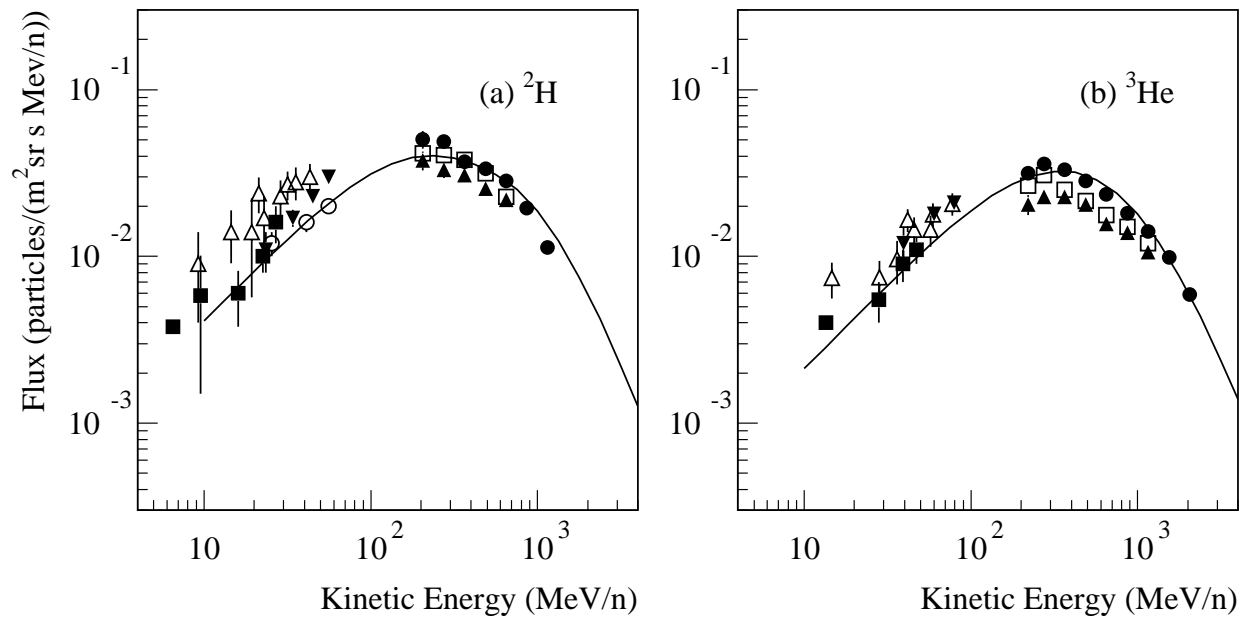


Figure 3: Differential energy spectra of (a) ^2H and (b) ^3He from BESS 93 (filled upward pointing triangles), BESS 94 (open squares) and BESS 95 (filled circles) along with other experimental data: filled downward pointing triangles, Beatty (1986); filled squares, Mewaldt, Stone, & Vogt (1976); open upward pointing triangles, Webber & Yushak (1983); open circles, Garcia-Munoz, Mason, & Simpson (1975); and calculated spectra (curves).

Acknowledgments

This work was supported in Japan by Grant-in-Aid for Scientific Research, Monbusho; and in USA by NASA grants NAGW-3526 and NAG 5-5061. We thank NSBF for balloon flight support. We also thank Dr. Tripathi R. K. at LaRC/NASA for his work on the LaRC model improvement based on our compiled cross section data.

References

- Beatty, J.J. 1986, *ApJ*, 311, 425
 Blinov, A.V., et al. 1984, *Soviet J. Nucl. Phys.*, 39, 161
 ———. 1985, *Soviet J. Nucl. Phys.*, 42, 133
 Carlson, R.F., 1996, *Atomic Data & Nucl. Data Tables*, 63, 93
 Davis, A.J., et al. 1995, *Proc. 24th ICRC (Rome, 1995)*, 2, 622
 Garcia-Munoz, M., Mason, G.M., & Simpson, J.A. 1975, *Proc. 14th ICRC (Munich)*, 1, 319
 Glagolev, V.V., et al. 1993, *Z. Phys. C*, 60, 421
 Jaros, J., et al. 1978, *Phys. Rev. C*, 18, 2273
 Meyer, J.P. 1972, *A&AS*, 7, 417
 Mewaldt, R.A., Stone, E.C., & Vogt, R.E. 1976, *ApJ*, 206, 616
 Moiseev, A., et al. 1997, *ApJ*, 474, 479
 Seo, E.S., et al. 1997, *Adv. Space Res.*, 19, 5, 751
 Seo, E.S., et al. 1998, *Adv. Space Res.*, in press
 Tripathi, R.K., Cucinotta, F.A. & Wilson, J.W. 1996, *Nucl. Instr. Meth. B*, 117, 347
 Webber, W.R., & Yushak, S.M. 1983, *ApJ*, 275, 391
 Yoshimura, K. et al. 1995, *Phys. Rev. Lett.*, 75, 3792